Quantum Electronics **36** (5) 447 – 456 (2006)

LASER BEAMS

PACS numbers: 42.60.Da; 42.62.Eh; 42.55.Lt
DOI: 10.1070/QE2006v036n05ABEH013244

Amplitude – phase mode structure of an astigmatic Gaussian beam in ring lasers with a nonplanar four-mirror cavity and an aperture

Yu.Yu. Broslavets, T.E. Zaitseva, A.A. Kazakov, A.A. Fomichev

***Abstract*. The structure of the fundamental mode field in a nonplanar ring four-mirror resonator with an aperture is determined taking into account rotations of the amplitude and phase distributions of an astigmatic Gaussian beam. The rotation angles of the axes of these distributions are calculated upon variations in the characteristic aperture size and the angle of curvature (nonplanarity) of the resonator. The effect of the resonator aperture and nonplanarity on the intensity distribution of the interference pattern behind a mixer is studied. It is shown that interference fringes have a slope depending on the orientations of the amplitude and phase distributions of the mode.**

Keywords: *nonplanar ring resonator, astigmatic Gaussian beam, ring laser*.

1. Introduction

Ring lasers are widely used in various laser devices, in particular, gyros. Planar ring resonators have been most thoroughly studied to date. The characteristics of modes in such resonators can be much easily determined than in nonplanar resonators due to their symmetry and the possibility to describe separately the mode structure of radiation in the resonator plane and in the perpendicular plane. In nonplanar resonators, the transverse structure of the beam field rotates around the optical axis of the resonator and a more complicated mode structure is formed [1]. The amplitude and phase distributions in the beam cross section can rotate through different angles in free space regions in such resonators, which can be used for obtaining a more homogeneous field [2, 3]. One of the most important applications of nonplanar resonators is their use in multifrequency gyros having the best accuracy to date [4, 5].

The theory of ring nonplanar resonators was developed in many papers [2, 5 – 10]. In [6], the spatial field distribution, polarisation, and the frequency spectrum of a cavity were determined. In [7], resonators with selecting elements were considered, in which beams with a complex astigmatism are formed. Nonplanar resonators were calculated by the ray method in [8]. The polarisation properties of a solid-state nonplanar resonator were investigated in [9]. A convenient approach for practical calculations of nonplanar resonators was proposed in [10], where a systematic analysis allowing one to determine the required parameters of modes in a nonplanar resonator was presented. Important calculations of ring resonators were performed in papers [11 – 14].

Despite a great number of papers devoted to nonplanar ring resonators, the questions related to the influence of the beam-image rotation on the interference pattern in the optical mixer of gyros with such a resonator and to the optimisation and selection of the optical scheme of a nonplanar resonator providing the most stable interference pattern and, eventually, the best accuracy of the gyro have not been adequately studied so far. It is also interesting to analyse various configurations of the resonator, both with the image rotation in a free space and without rotation, but with the 90° turn of the field in the cross section per round trip in the resonator. In addition, of interest is the effect of the resonator aperture on the intensity distribution in the interference pattern behind the mixer.

In this paper, we considered a symmetrical nonplanar four-mirror resonator in which all the angles of incidence on mirrors are identical and are determined by the angle of curvature (nonplanarity) of the resonator, which is selected so that the rotation of the plane of incidence of the mode beam on passing from one mirror to another would be 22.5°. The resonator sides had the same length. A spherical mirror providing the resonator stability was mounted opposite to the output mirror. Due to its high symmetry and the rotation of the field in the beam cross section through 90° per round trip in the resonator, such a resonator is quite stable and at the same has no additional intracavity elements providing the operation of a gyro but introducing additional errors. In the nonplanar resonator, the counter-propagating beams with a circular polarisation are generated, which allows the use of the Zeeman effect to produce a frequency bias.

In this paper, we studied the influence of variations in the resonator design on its mode structure and the intensity distribution in the interference pattern at the output of a mixer taking into account the rotation of the amplitude and phase distributions of an astigmatic Gaussian beam. We obtained equations for calculating the parameters of a beam propagating in a nonplanar resonator and determining the mode structure of radiation. A scalar model was considered

Yu.Yu. Broslavets, T.E. Zaitseva, A.A. Fomichev Moscow Institute of Physics and Technology (State University), Institutskii per. 9, 141700 Dolgoprudnyi, Moscow region, Russia; e-mail: laser@pop3.mipt.ru;
A.A. Kazakov M.F. Stel'makh Polyus Research & Development Institute, ul. Vvedenskogo 3, 117342 Moscow, Russia

Received 27 October 2005
Kvantovaya Elektronika **36** (5) 447 – 456 (2006)
Translated by M.N. Sapozhnikov

by neglecting radiation polarisation. All the calculations were performed assuming that only the fundamental transverse mode was generated in the resonator.

2. Theoretical description of a nonplanar four-mirror resonator

The field in an astigmatic Gaussian beam can be described in the coordinate system coupled to the axes of the beam distribution in the cross section by the expression [10, 15–17]

$$U = \frac{G}{[q_1 q_2]^{1/2}} \exp\left[-\frac{ik}{2}\left(\frac{x^2}{q_1}+\frac{y^2}{q_2}\right) - ikz + i\phi\right], \quad (1)$$

where

$$\frac{1}{q_1} = \frac{1}{R_1} - i\frac{\lambda}{\pi\omega_1^2}; \quad \frac{1}{q_2} = \frac{1}{R_2} - i\frac{\lambda}{\pi\omega_2^2};$$

q_1 and q_2 are the complex parameters of the beam; x, y, z are the transverse and longitudinal coordinates, respectively; G is the field amplitude; $k = 2\pi/\lambda$; λ is the radiation wavelength; R_1 and R_2 are the radii of curvature of wave fronts; ω_1, and ω_2 are the cross sections of the beams in mutually perpendicular directions; and ϕ is the initial phase. In the beam defined in this way, the principal axes of the amplitude and phase distributions coincide and are directed along the coordinate axes, while the beam is described by the complex parameters $q_1(z)$ and $q_2(z)$ determining the transverse size and the curvature of the wave front of the beam in the planes xz and yz, respectively. The difference between the complex parameters in perpendicular planes determines the beam astigmatism. When these parameters are equal, the beam becomes a usual non-astigmatic Gaussian beam.

Consider the representation of an astigmatic beam in the coordinate system rotated through an angle around the longitudinal axis. In this case, we can write for new coordinates:

$$\begin{pmatrix} x' \\ y' \end{pmatrix} = F\begin{pmatrix} x \\ y \end{pmatrix}, \quad (2)$$

where

$$F = \begin{pmatrix} \cos\varphi & -\sin\varphi \\ \sin\varphi & \cos\varphi \end{pmatrix}$$

is the matrix of rotation of a new coordinate system (x', y') through the angle φ with respect to the old system (x, y). The first term of the sum in the exponent (by omitting $-ik/2$) describing the field of expression (1), representing a quadratic form, can be written in the matrix form

$$\frac{x^2}{q_1}+\frac{y^2}{q_2} = (x,y)P\begin{pmatrix} x \\ y \end{pmatrix}, \quad (3)$$

where

$$P = \begin{pmatrix} \frac{1}{q_1} & 0 \\ 0 & \frac{1}{q_2} \end{pmatrix}.$$

In this case, by rotating the coordinate system through the angle φ, the quadratic form can be written as

$$\frac{x^2}{q_1}+\frac{y^2}{q_2} = (x,y)F^{-1}FPF^{-1}F\begin{pmatrix} x \\ y \end{pmatrix} = (x',y')T\begin{pmatrix} x' \\ y' \end{pmatrix}, \quad (4)$$

where

$$F^{-1}(\varphi) = \begin{pmatrix} \cos\varphi & \sin\varphi \\ -\sin\varphi & \cos\varphi \end{pmatrix}; \quad (5)$$

$$T = FPF^{-1} = \begin{pmatrix} a & b \\ b & c \end{pmatrix}; \quad (6)$$

$$a = \frac{\cos^2\varphi}{q_1}+\frac{\sin^2\varphi}{q_2}; \quad b = \left(\frac{1}{q_1}-\frac{1}{q_2}\right)\sin\varphi\cos\varphi;$$

$$c = \frac{\sin^2\varphi}{q_1}+\frac{\cos^2\varphi}{q_2}. \quad (7)$$

Thus, the field of the astigmatic Gaussian beam in the coordinate system turned through the angle φ with respect to the system axes, in which the quadratic form has the canonical form, can be represented in the form

$$U = \frac{G}{(q_1 q_2)^{1/2}} \exp\left[-\frac{ik}{2}(ax'^2 + 2bx'y' + cy'^2) - ikz + i\phi\right]. \quad (8)$$

In this case, the beam is defined by the coefficients of the matrix

$$T = \begin{pmatrix} a & b \\ b & c \end{pmatrix}. \quad (9)$$

If the angle of rotation $\varphi = \varphi_r + i\varphi_i$ of the coordinate system in the matrix transformation is written in the complex form assuming that the rotation of the system through a complex angle is some matrix transformation (4)–(7), the obtained representation of the astigmatic beam will describe the beams in which the amplitude and phase distributions are turned with respect to each other and the coordinate system. In this case, the elements of the matrix T will be complex. To find the complex parameters of the beam in such a representation, it is necessary to pass to the coordinate system in which the imaginary or real part of the quadratic form will not have the diagonal term, i.e., $\mathrm{Im}b = 0$ or $\mathrm{Re}b = 0$. In this case, the radii of curvature of the wave front or the beam cross section are determined from the coefficients of the quadratic form in the canonical representation.

The angles of rotation ξ and η of the phase and amplitude distributions of the coordinate system in which the quadratic form will have the canonical form of the corresponding distribution with respect to the initial coordinate system can be determined from the relations

$$\xi = \frac{1}{2}\arctan\frac{2b'}{a'-c'}, \quad (10)$$

$$\eta = \frac{1}{2}\arctan\frac{2b''}{a''-c''}. \quad (11)$$

In the vicinity of points where $a' = c'$ or $a'' = c''$, we have

$$\xi = \delta\frac{1}{2}\arccos\left\{\delta\frac{a'-c'}{[(a'-c')^2+4b'^2]^{1/2}}\right\}\operatorname{sign} b',$$
$$\eta = \varepsilon\frac{1}{2}\arccos\left\{\varepsilon\frac{a''-c''}{[(a''-c'')^2+4b''^2]^{1/2}}\right\}\operatorname{sign} b''. \quad (12)$$

Here, $a = a' + ia''$, $b = b' + ib''$, and $c = c' + ic''$ are the coefficients of the quadratic form of the matrix T represented by the imaginary and real parts; $\delta = \pm 1$; $\varepsilon = \pm 1$. The signs δ and ε are determined by the initial orientation of the axes of distributions with respect to the coordinate system because there exists some ambiguity in the determination of the angle of rotation of the second-order curve. By reducing this curve to the canonical form, it can be turned through an angle with an accuracy of $\pm\pi/2$, which does not allow one to determine uniquely the directions of the major and minir semiaxes. To eliminate this ambiguity, information on the initial direction of axes is required.

Thus, knowing the matrix T specifying the astigmatic Gaussian beam and reducing its imaginary or real part to the diagonal form by rotating the coordinate system through the angle $-\xi$ (for the real part) or angle $-\eta$ (for the imaginary part), we determine the transverse size of the beam or curvature of the wave front for the given beam cross section:

$$T_r = F^{-1}(-\xi)\,\mathrm{Re}\,TF(-\xi) = \begin{pmatrix} A_r & 0 \\ 0 & B_r \end{pmatrix}, \quad (13)$$

$$T_i = F^{-1}(-\eta)\,\mathrm{Im}\,TF(-\eta) = \begin{pmatrix} A_i & 0 \\ 0 & B_i \end{pmatrix}, \quad (14)$$

$$\omega_1 = \left(-\frac{\lambda}{\pi A_i}\right)^{1/2},\ \omega_2 = \left(-\frac{\lambda}{\pi B_i}\right)^{1/2},$$
$$R_1 = \frac{1}{A_r},\ R_2 = \frac{1}{B_r}. \quad (15)$$

Consider the transformation of the matrix T in individual elements of the resonator: mirrors, free space regions, and the aperture. After the propagation of the beam through a free space region of length z, this transformation can be written in the form

$$T' = (E + zT)^{-1}T,$$

where

$$E = \begin{pmatrix} 1 & 0 \\ 0 & 1 \end{pmatrix} \quad (16)$$

is the unit matrix.

The transformation of the matrix T on passing to the coordinate system coupled to the plane of incidence of the beam on the next mirror is obtained by rotating the coordinate system through the angle φ corresponding to the angle between the planes of incidence of the beam on successively mounted mirrors. In this case, the direction of rotation should be opposite to the direction of rotation of the planes of incidence:

$$T' = F^{-1}(\varphi)\,TF(\varphi). \quad (17)$$

The transformation of the matrix T upon reflection of the beam from a mirror and performed because it is necessary to select the right-hand orientation of the direction vectors of the coordinate system has the form

$$T' = MTM,$$

where

$$M = \begin{pmatrix} -1 & 0 \\ 0 & 1 \end{pmatrix}. \quad (18)$$

The propagation of an astigmatic Gaussian beam through a quadratic corrector is described in the general case by multiplying the field distribution function by the factor

$$U'(x,y,z) = U(x,y,z)S(x,y), \quad (19)$$

where

$$S(x,y) = \exp\left[\frac{ik}{2}(Ax^2 + 2Bxy + Cy^2)\right]; \quad (20)$$

A, B, and C are the coefficients, which are complex in the general form and can describe both the phase and amplitude correction, which is equivalent to that produced by an astigmatic lens, a spherical mirror or an astigmatic aperture. The matrix describing a quadratic corrector in the general case has the form

$$K = \begin{pmatrix} A & B \\ B & C \end{pmatrix},$$

while the transformation of the matrix T corresponding to the astigmatic beam in the quadratic corrector is

$$T' = T + K. \quad (21)$$

The transformation of the beam incident and reflected at an angle of $\gamma/2$ from a spherical mirror with the radius of curvature R is described by the relation

$$T' = T + K_1, \quad (22)$$

where

$$K_1 = \begin{pmatrix} -\dfrac{2}{R\cos(\gamma/2)} & 0 \\ 0 & -\dfrac{2\cos(\gamma/2)}{R} \end{pmatrix}, \quad (23)$$

and the transformation of the beam matrix T after propagation through a Gaussian aperture can be written in the form

$$T' = T + K_2, \quad (24)$$

where K_2 is the matrix describing the quadratic correction of the beam propagated through a Gaussian elliptic aperture. Because a circular aperture was used in the resonator under study, its dimensions Δ_a and Δ_c along the x and y axes are the same. In this case, K_2 is determined from the expression

$$K_2 = \begin{pmatrix} -\dfrac{i\lambda}{\pi\Delta_a^2} & 0 \\ 0 & -\dfrac{i\lambda}{\pi\Delta_c^2} \end{pmatrix}, \quad (25)$$

where λ is the radiation wavelength and $\Delta_a = \Delta_c = \Delta$ is the aperture radius.

Consider a non-planar four-mirror resonator (Fig. 1) with one spherical and three plane mirrors. Output mirror M1 is located opposite to spherical mirror M3. Aperture D is place in front of the output mirror. We assume that the optical scheme is symmetric, i.e., all the arms of the resonator are identical: $AB = BC = CD = DA = L$. The angles of incidence of the beam on mirrors and angles between the planes BAD, ADC, DCB, and CBA equal to φ in modulus are also identical and are determined by the angle of nonplanarity β of the resonator.

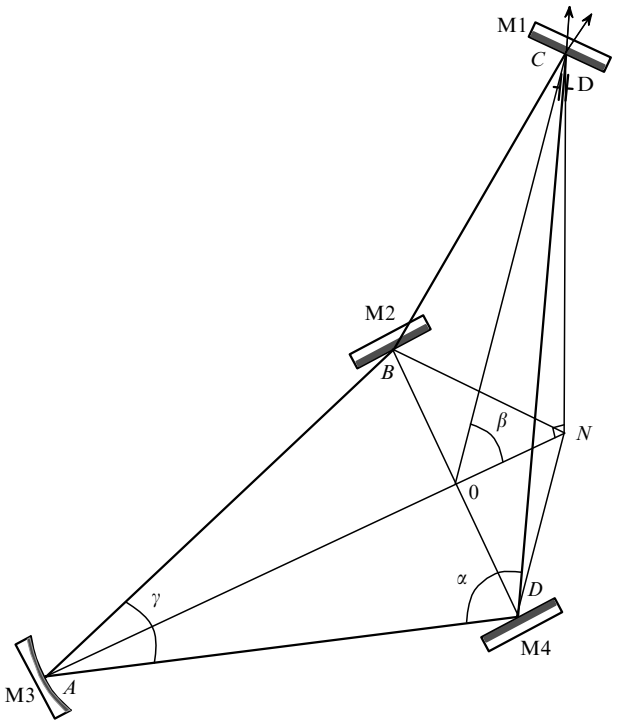

Figure 1. Optical scheme of the nonplanar resonator of a laser gyro.

For a symmetric nonplanar resonator with equal sides and angles of incidence on mirrors, the angle of nonplanarity β and the angle of rotation φ of the plane of incidence of the beam from one mirror to another are related by the expression

$$\cos^2(\beta/2) = \cos\varphi. \tag{26}$$

The relation between the angle of incidence $\gamma/2$ and angle φ has the form

$$\tan^2(\gamma/2) = \cos\varphi. \tag{27}$$

For an asymmetric resonator, when the angles of incidence on mirrors are different, i.e., $\gamma/2 \neq \alpha/2$, the relations

$$\cos\varphi = \tan(\gamma/2)\tan(\alpha/2), \tag{28}$$

$$\sin\varphi \sin\alpha = \cos(\gamma/2)\sin\beta \tag{29}$$

are fulfilled.

Let us find the transformation of the beam matrix T in each arm of the resonator taking into account the rotation of the plane of incidence from one mirror to another and the reorientation of the coordinate system at which the direction basis becomes right-hand oriented after reflection from a mirror. In this case, it should be taken into account that the angle φ between the planes of incidence on mirrors changes its sign on passing from one mirror to another. As the initial plane, we will use an incident plane of the beam behind mirror M1 assuming that the beam propagates in the resonator counter-clockwise. The x' axis in the coordinate system $x'y'z$ is located in the initial plane, the z axis is directed along the beam, and the y' axis is directed perpendicular to the initial plane, providing the right-hand orientation of the coordinate system. As a result, we obtain the matrix transformation for the initial beam described by the matrix T_1 upon a round trip in the resonator:

$$\begin{aligned}
T_2 &= M F^{-1}(-\varphi)\left[(E + z\,T_1)^{-1}\,T_1\right] F(-\varphi)\,M,\\
T_3 &= M F^{-1}(\varphi)\left[(E + z\,T_2)^{-1}\,T_2 + K_1\right] F(\varphi)\,M,\\
T_4 &= M F^{-1}(-\varphi)\left[(E + z\,T_3)^{-1}\,T_3\right] F(-\varphi)\,M,\\
T_5 &= M F^{-1}(\varphi)\left[(E + z\,T_4)^{-1}\,T_4 + K_2\right] F(\varphi)\,M,\\
T_1 &= T_5,
\end{aligned} \tag{30}$$

where T_2 is the matrix describing the astigmatic Gaussian beam after propagation through free region CB and reflection from mirror M2; T_3 is the beam matrix after propagation through free region BA and reflection from spherical mirror M3; T_4 is the beam matrix after propagation through free region AD and reflection from mirror M4; T_5 is the beam matrix after propagation through free region DC and aperture and refection from mirror M1; z is the coordinate measured from the point of incidence of the beam on the mirror to the section in the beam in the resonator arms or equal to L upon complete propagation through the arm.

Similar transformations can be obtained for a counter-propagating beam. Assuming that after a round trip in the resonator, the beam arrives at the initial plane of the section and then, after multiple round trips, a stationary field distribution is established in the resonator, we can find both the stationary parameters of the beam and their variation during the establishment process. For this purpose, we assign to the initial matrix T_1 the values of the matrix T_5 obtained due to transformations in equations for the entire resonator.

3. Numerical calculation of a nonplanar resonator with one spherical mirror

The matrix recurrent equations obtained in the paper were solved numerically. As the initial approximation, a family of matrices T_1 was formed which determined a number of astigmatic beams having in the general form the amplitude and phase distributions turned, according to (2), through different angles with respect to the coordinate system. As the initial approximation, the complex parameters q_1 and q_2 were calculated for a similar but planar resonator. After multiple transformations in recurrent equations (30), the

initial matrices T_1 were reduced to stationary matrices determining the distribution of the mode field for the specified parameters of the resonator.

The characteristic establishment times of a stationary mode were determined by the aperture size. Figure 2 shows the dependence of establishment of the transverse size of the beam on the number of round trips in the resonator. For the resonator perimeter length $4L = 0.2092$ m and the aperture $\Delta = 0.00053$ m, the mode establishment time was 15 ns, and for the aperture $\Delta = 0.001$ m, it was ~ 50 ns.

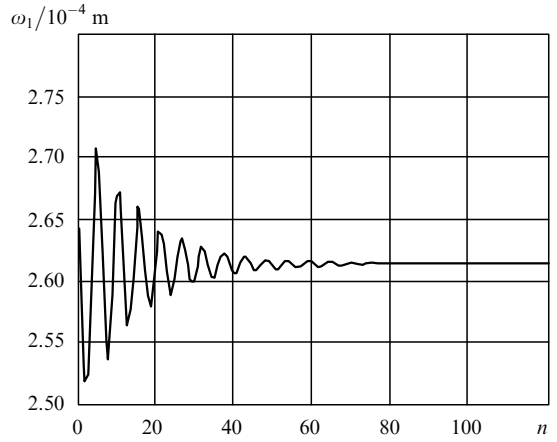

Figure 2. Transverse size ω_1 of the beam along the x axis as a function of the number n of round trips in the resonator with the aperture $\Delta = 0.001$ m (behind the output mirror).

We calculated a nonplanar resonator for a helium – neon Zeeman laser gyro with the following parameters: the resonator is completely symmetric over angles and arms lengths, the radiation wavelength is $\lambda = 0.6328$ μm, the resonator arm length is $L = 0.0523$ m, the aperture size is $\Delta = 0.00053$ m, the radius of curvature of the spherical mirror is $R = 1.36$ m, the angle of nonplanarity $\beta = 32.03124^\circ$ corresponds to the angle $\varphi = 22.5^\circ$, and the angle of incidence of the beam on mirrors is $\gamma/2 = 43.86622^\circ$.

Figures 3a, b show the transverse dimensions of the beam in the orthogonal directions along the x and y axis in the resonator cross section in front of the output mirror and after reflection from it calculated as functions of the distance z from the output mirror. At a distance of 10 cm from the output mirror, the beam dimensions are $\omega_1 = 281.5$ μm and $\omega_2 = 265.6$ μm, and $\omega_1 = 248.5$ μm and $\omega_2 = 247.4$ μm on the output mirror (here ω_1 and ω_2 are the beam size along the x and y axes, respectively). Because the aperture is placed in front of the output mirror in the resonator, the beam size in each orthogonal direction is characterised by the two dependences: the upper one, corresponding to the beam size in front of the aperture on the interval $[-0.1; 0]$ (in the absence of the aperture, the dependence would continue on the interval $[0; 0.1]$), and the lower one, corresponding to the beam size behind the aperture on the interval $[0; 0.1]$ and the continuation of the dependence of the beam size on the interval $[-0.1; 0]$. Thus, the beam dimensions sharply change at the point $z = 0$ after its propagation through the aperture. The dimensions of the beam cross section are shown in the coordinate system coupled with the principal axes of the amplitude distribution. These dependences demonstrate that beam waists in orthogonal directions are displaced from the output to spherical mirror and are located asymmetrically. Figures 3c, d show the dependences of the inverse curvature $1/R$ of the wave front of the beam on the distance from the output mirror. On the interval $[-0.1; 0]$ (Figs 3c, d), it is necessary to take into account the upper dependence, as well as on the $[0; 0.1]$ interval. For convenience of the consideration, the dependences are continued beyond the origin of reference.

It was found in numerical simulations that after the establishment of the mode structure in the resonator, the mode parameters were independent of the initial parameters of a family of beams taken with different angles between the amplitude and phase distributions. Thus, irrespective of the initial parameters of the beam, the established distribution of the field was determined by the resonator parameters. The phase distribution is shown in Fig. 4. The amplitude field distribution in the beam cross section on the output mirror is well described by a Gaussian distribution. A noticeable astigmatism of the phase distribution was

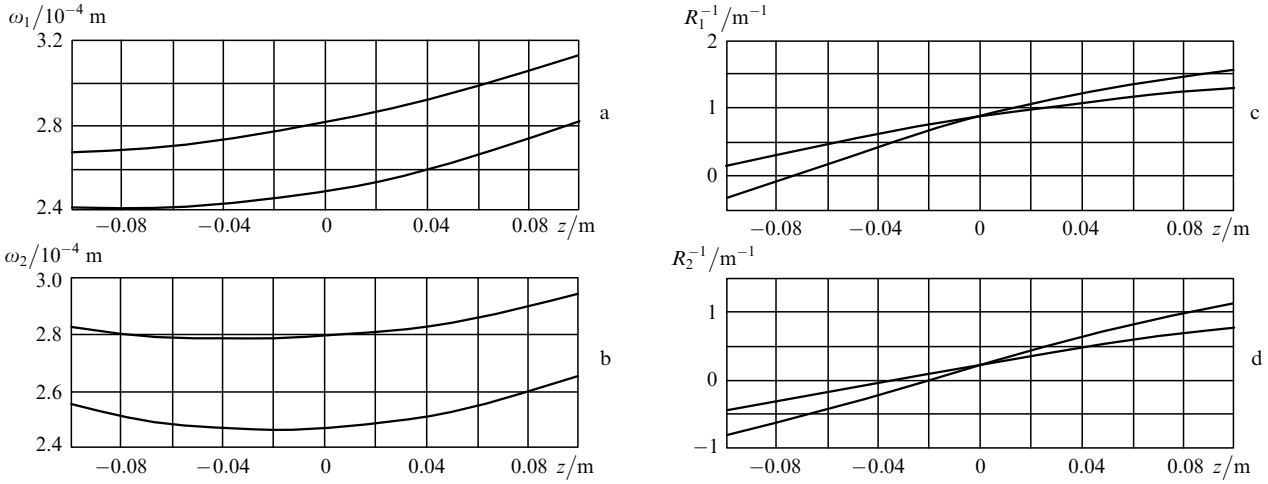

Figure 3. Transverse sizes ω_1 and ω_2 of the beam in directions x (a) and y (b), respectively, as functions of the distance z from the output mirror for $\Delta = 0.00053$ m and the dependences of the wave-front curvature R_1^{-1} and R_2^{-1} of the beam before and after reflection from the output mirror in directions x (c) and y (d).

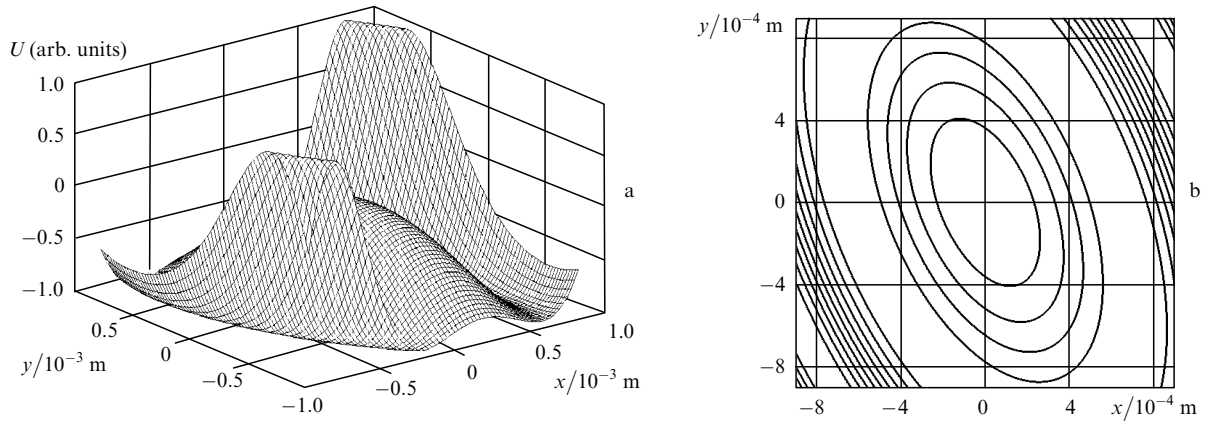

Figure 4. Dependences of the phase factor of the field in the beam cross section (a) and equal-phase cross sections in the phase distribution of the beam (b) on the output mirror.

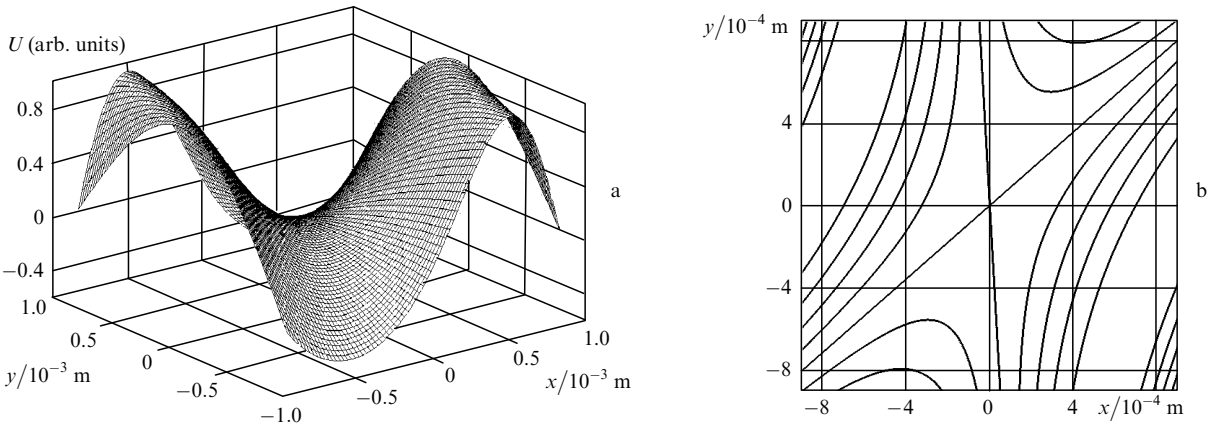

Figure 5. Dependences of the phase factor of the field in the beam cross section (a) and equal-phase cross sections in the phase distribution of the beam (b) behind the spherical mirror.

observed, while the astigmatism of the amplitude distribution was rather small. This is caused by the rotation of the beam image through 90° during a round trip in the resonator. In the region between waists in the resonator, the curvature of the wave front along different axis has different signs. As a result, the phase distribution of the transverse structure (the second-order surface near the beam axis) is a hyperbolic paraboloid. For this reason, the distribution of the phase factor in the beam cross section behind the spherical mirror has the shape shown in Fig. 5, while the amplitude distribution has a noticeable astigmatism.

One of the factors affecting the gyro parameters is the transverse mode structure of the field. In most gyros, attempts are made to provide the conditions for generation of the fundamental mode of the Gaussian distribution, although interesting results demonstrating the possibility of removing frequency locking upon generation of higher-order modes were obtained in some papers [18]. The numerical simulation performed in our paper showed that, as the aperture size was changed, the structure of an astigmatic beam in the resonator considerably changed, and its waists in orthogonal directions displaced toward the spherical mirror with decreasing the aperture size. In the absence of the aperture, the eigenmode of the resonator is an astigmatic beam with waists in mutually orthogonal directions located symmetrically at the same distances from the output mirror: one – before reflection [curve (*1*) in Fig. 6a] and another – after [curve (*2*) in Fig. 6b]. As the aperture size is reduced, the waists move from the output mirror to

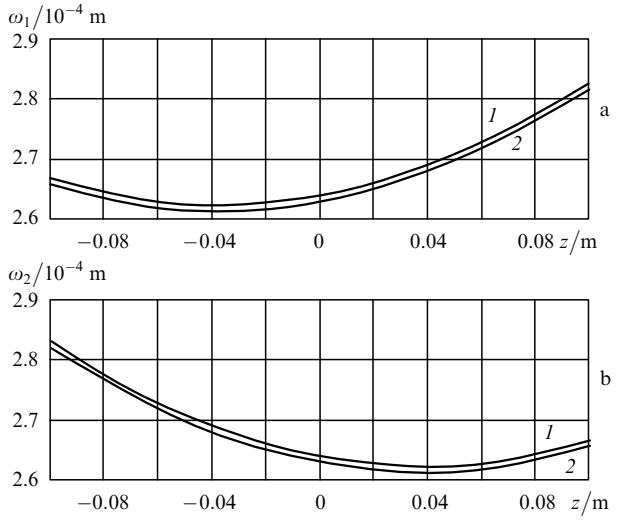

Figure 6. Transverse sizes of the beam in directions x (a) and y (b) as functions of the distance z from the output mirror for the aperture $\Delta = 0.003$ m.

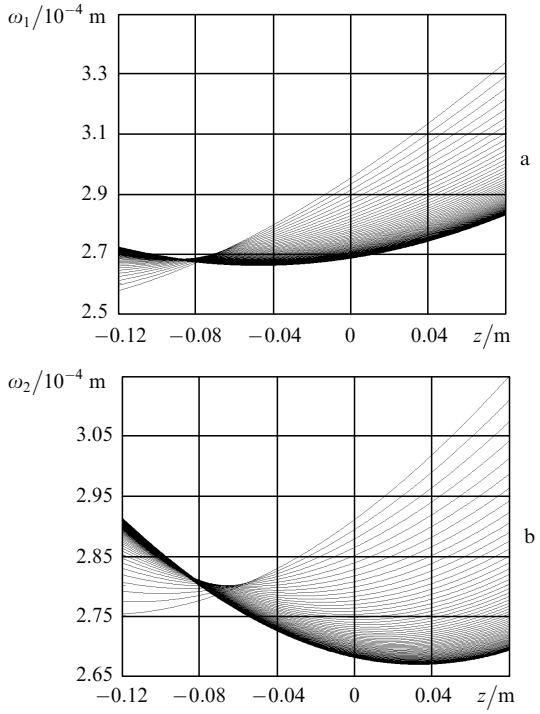

Figure 7. Family of curves describing transverse sizes $\omega_1(z)$ and $\omega_2(z)$ of the beam in directions x (a) and y (b), respectively, in different cross sections of the resonator for different aperture sizes. The distance z is measured from the output mirror. The negative and positive values of z correspond to the distances in front of and behind the mirror, respectively. Curves with waists located closer to zero correspond to a larger aperture.

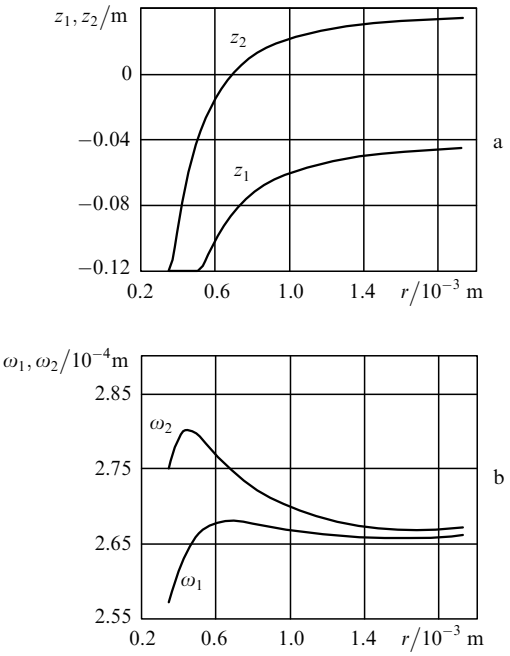

Figure 8. Positions z_1 and z_2 of waists (a) and their sizes ω_1 and ω_2 (b) in the resonator as functions of the aperture radius r. The lower and upper curves are the dependences in the directions x and y, respectively. Distances z_1 and z_2 are measured from the output mirror (negative and positive values correspond to positions in front of and behind the mirror, respectively).

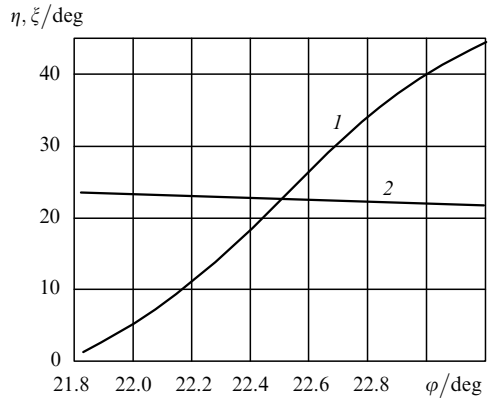

Figure 9. Slopes of the amplitude-distribution axis η (*1*) and phase-distribution axis ξ (*2*) in the cross section on the output mirror as functions of the rotation angle φ of the plane of incidence of the beam.

the spherical one (Figs 7, 8). As a result, both waists enter the spherical mirror region, and their size first increases with decreasing the aperture size and then, having achieved a maximum, begins to strongly decrease (Fig. 8). Note also that because the aperture is located on the output mirror, the dependences in Fig. 7 for positive distances are qualitative. In reality, the beam size sharply changes after propagation through the aperture. Thus, the reduction of the aperture size leads to the increase in the beam astigmatism (Figs 7, 8). Therefore, to reduce the beam astigmatism, the aperture size should be chosen so that the waist size would not achieve a maximum.

The calculation of the slopes of axes of the amplitude and phase distributions as functions of the angle of non-

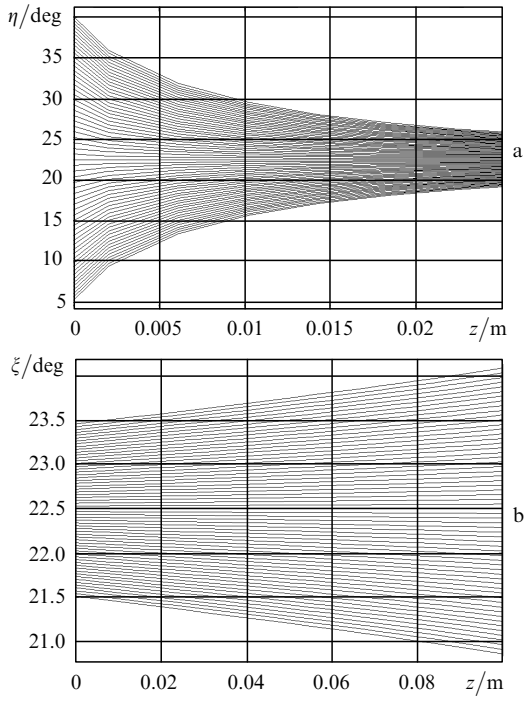

Figure 10. Family of curves η (a) and ξ (b) during propagation of the beam behind the output mirror in free space.

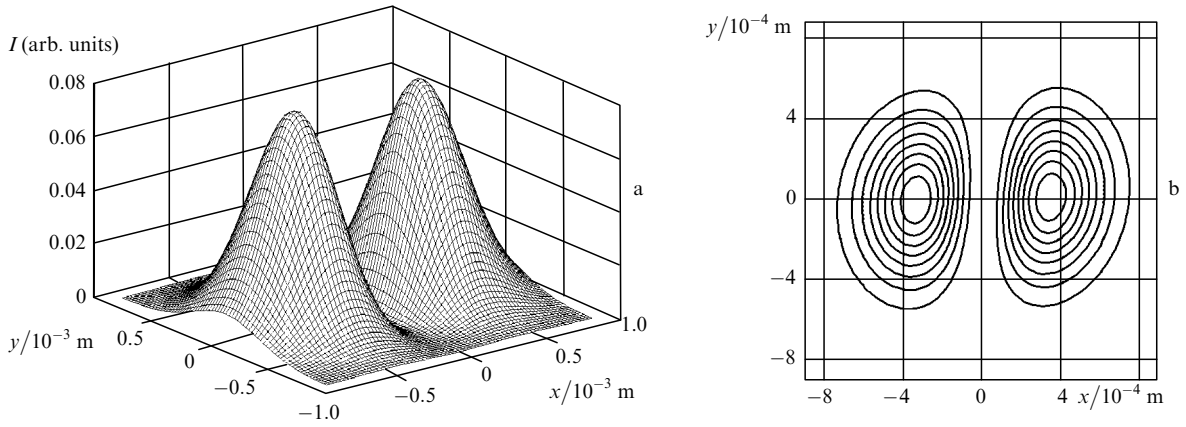

Figure 11. Intensity distribution (a) and equal-intensity lines (b) in the interference pattern at the mixer output.

planarity of the resonator showed a considerable change in the slope of the amplitude distribution (Fig. 9). We considered small deviations from the angle of nonplanarity, which provided the rotation of the plane of incidence through the angle $\varphi = 22.5^\circ$ on passing to the next arm of the resonator.

Figure 10 shows the calculated dependences of the turn of the amplitude [$\eta(z)$] and phase [$\xi(z)$] distributions of a beam in the resonator propagating behind the output mirror. Each of the curves corresponds to a certain angle of nonplanarity of the resonator. A considerable rotation of the axes of the amplitude distribution is observed, and at the same time there exists the angle of nonplanarity at which the axes are not rotated during the beam propagation. The amplitude distribution curves arranged from bottom to top correspond to the increase in the angle of nonplanarity, while the phase distribution curves arrange in the same order correspond to the decrease in this angle.

Figure 11 shows the intensity distribution in the interference pattern at the output of the laser gyro mixer calculated for the resonator under study. The dip observed between the beams corresponds to the minimum of the interference fringe intensity. The beams are combined so that their overlap region corresponds approximately to one third of the intensity of each of the beams.

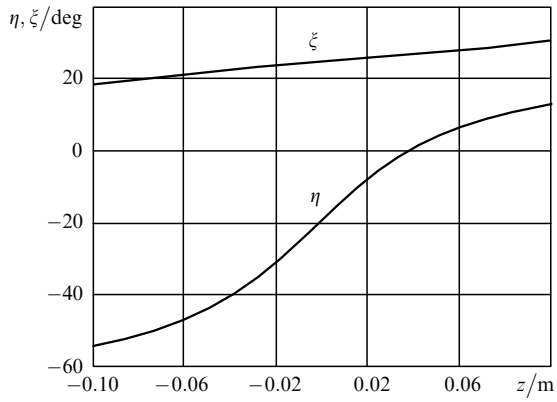

Figure 12. Dependences of the rotation angles η and ξ of the amplitude and phase distributions of the beam on the distance z from the output plane mirror.

4. Calculation of a nonplanar resonator with two spherical mirrors

Beams with the amplitude and phase distributions rotating during propagation in the free-space regions of the resonator can be formed in it not only upon the deviation of the angle of nonplanarity from the value providing the existence of the mode with an astigmatic beam without rotation of the field but also when more than one spherical mirrors are used. If two spherical mirrors located in the opposite arms of the resonator are used, a mode is formed

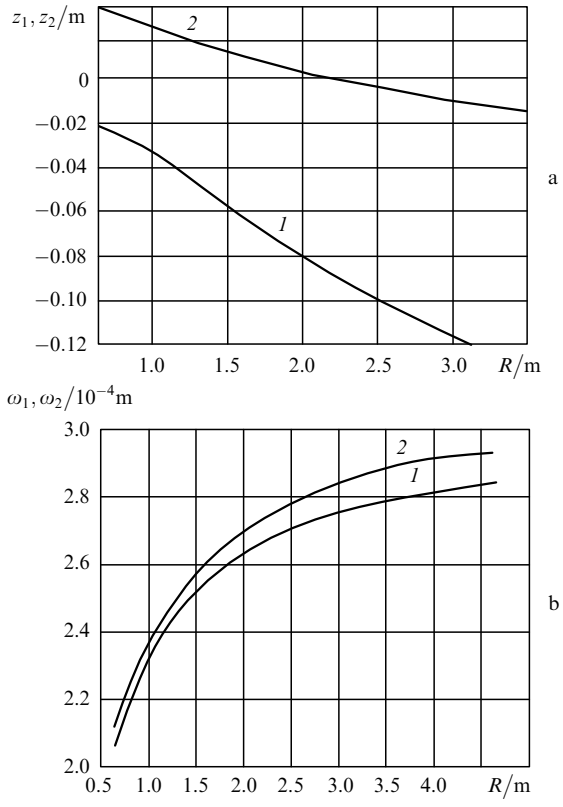

Figure 13. Dependences of the beam-waist positions with respect to the output mirror (a) and of the beam-waist sizes (b) in directions x (*1*) and y (*2*) on the radius of curvature of the spherical mirror varying simultaneously for two spherical mirrors of the resonator.

in which the amplitude and phase distributions rotate in the free-space regions. The rotation of the axes of the amplitude and phase distributions during the beam propagation in a free space in the resonator arm is shown in Fig. 12. The radius of curvature of spherical mirrors was taken in calculations twice as large as that in the resonator with one mirror. Figure 13 shows the dependences of the position and size of the waist on the radius of curvature of mirrors.

Thus, a change in the curvature of plane mirrors, for example, upon their bending caused by the action of a piezoceramic motor of the perimeter control system can lead to the rotation of the phase and amplitude distributions of the beam.

5. Experimental measurement of the parameters of an astigmatic Gaussian beam

We measured the transverse distribution of the field at the output of an LGK-200 Zeeman laser gyro with a nonplanar resonator, whose parameters were determined above. The intensity distribution in the output-beam cross section shows that the beam has no astigmatism and is virtually circular. The dependences of the transverse intensity distributions measured in orthogonal directions at a distance of 10 cm behind the output mirror showed (Fig. 14) that the difference between measured and calculated waist sizes was smaller than 10 μm within the measurement error. The transverse dimensions of the beam $\omega_1 = 287$ μm and $\omega_2 = 271$ μm agree with the calculated values (Fig. 3) $\omega_1 = 281.5$ μm and $\omega_2 = 265.6$ μm.

The intensity distribution in the interference pattern shown in Fig. 15 was measured in the far-field zone at

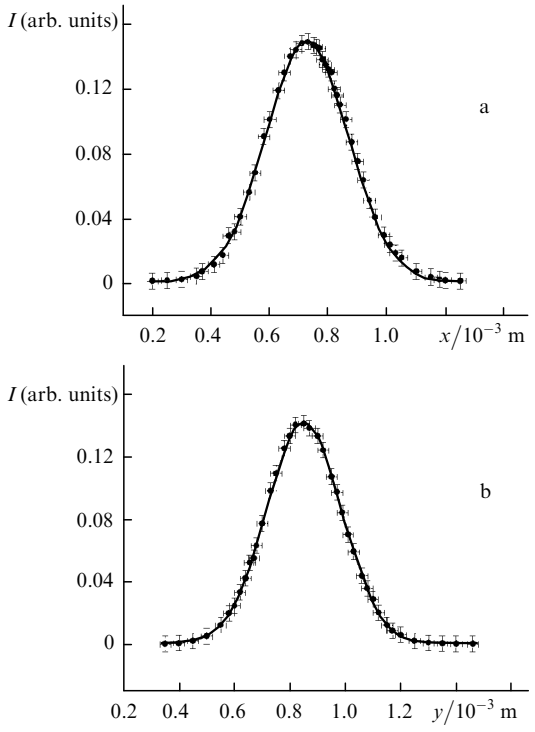

Figure 14. Dependences of the beam intensity on the transverse coordinates x ($\omega_1 = 287$ μm) (a) and y ($\omega_2 = 271$ μm) (b) measured behind the output mirror.

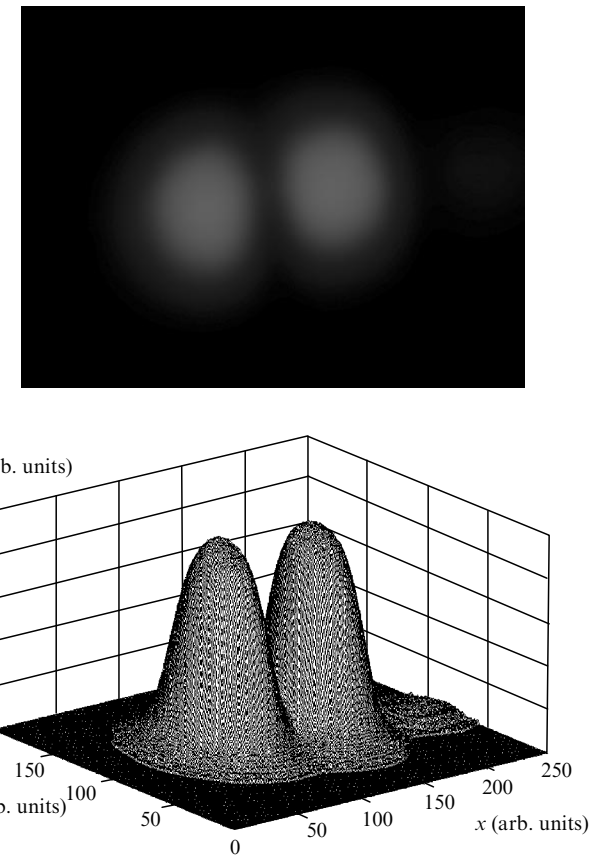

Figure 15. Intensity distribution upon the intersection of two beams at the mixer output. The dark band between the beams is the result of their interference.

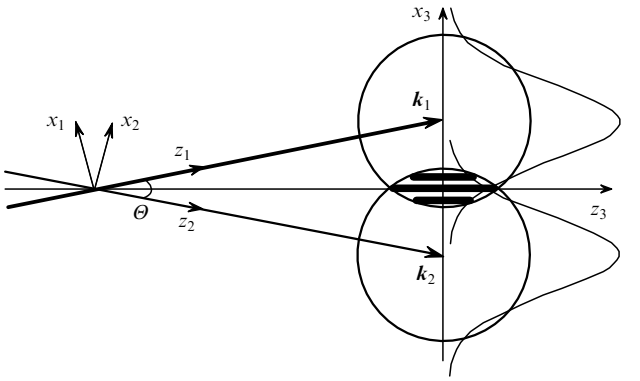

Figure 16. Direction of astigmatic Gaussian beams at the mixer output upon interference (Θ is the angle between the beams).

the output of a mixer providing the convergence of the beams at the required angle. The convergence angle Θ (Fig. 16) was chosen to obtain only one interference maximum or minimum in the overlap region of the beams. The intensity distributions obtained in this way revealed the presence of the slope of interference fringes (Fig. 15). The numerical simulations showed that the slope of interference fringes (Fig. 11) was determined by the turn of the phase distribution axes (Fig. 4). If the turn angle of the phase distribution is zero, the interference fringes prove to be perpendicular to the line connecting the axes of the beams.

Thus, the rotation of the phase distribution in the beam cross section leads to the slope of interference fringes, which

should be taken into account during the orientation of a photodetector.

6. Conclusions

We have used a simple method for describing nonplanar resonators based on quadratic matrices determining an astigmatic Gaussian beam. Despite its simplicity, this method allowed us to describe the field distribution in the resonator and calculate the main parameters of a mode such as the beam cross section, the wave-front curvature, and the rotation angles of the amplitude and phase distributions.

The numerical calculations have shown that in a nonplanar four-mirror resonator with one spherical mirror with the angle of nonplanarity chosen equal to 32.031236°, the mode is an astigmatic Gaussian beam without rotation of the field during propagation through free spaces. At the same time, the presence of angles between the plane of incidence on the resonator mirrors specified by the nonplanarity angle of the resonator leads to the rotation of the amplitude and phase distributions of the beam through 90° per round trip in the resonator. Such a configuration allows one to equalise efficiently the semiaxes of the amplitude distribution on the output mirror, and at the same time the phase distribution of the beam remains astigmatic.

A mode formed in a nonplanar resonator with a spherical mirror without an aperture has two waists in mutually orthogonal directions, which are located symmetrically at the same distance from the output mirror placed opposite to the spherical mirror. The use of an aperture on the output mirror leads to the displacement of the waists towards the spherical mirror, which increases with decreasing the aperture diameter.

The calculated rotation of interference fringes in the observation plane of the interference pattern taking place upon a change in the rotation angle of the semiaxes of the phase distribution was also observed in experiments with an LGK-200 Zeeman laser gyro during measurements of the intensity distribution in the interference pattern of two counterpropagating beams in the gyro.

In nonplanar resonators with rotating amplitude and phase distributions of the mode, it is necessary to take into account the slope of axes of these distributions in a mixer. The deviation of the angle of nonplanarity of the resonator from the value providing the rotation of the amplitude and phase distributions through 90° per round trip in the resonator leads to the formation of beams with rotation of the axes of amplitude and phase distributions observed in their cross sections in certain regions of the resonator.

The field distribution calculated for a nonplanar resonator with two spherical mirrors revealed the presence of a mode with rotating amplitude and phase distributions in the free-space regions of the resonator.

Our study has shown that the mode of a nonplanar four-mirror resonator with one spherical mirror is an astigmatic Gaussian beam in which the rotation of the axes of amplitude and phase distributions through different angles is observed in the general case, which results in the redistribution of the structure of the interference pattern and rotation of interference fringes. To improve the accuracy and stability of a laser gyro, this rotation should be taken into account in the gyro mixer.

Acknowledgements. This work was supported by the Russian Foundation for Basic Research (Grant No. 05-02-08113).

References

1. Anan'ev Yu.A. *Opticheskie rezonatory i problema raskhodimosti lazernogo rezonatora* (Optical Resonators and the Problem of Divergence of a Laser Resonator) (Moscow: Nauka, 1979).
2. Golyaev Yu.D., Evtyukhov K.N., Kaptsov L.N., Smyshlyaev S.P. *Kvantovaya Elektron.*, **8**, 2321 (1981) [*Sov. J. Quantum Electron.*, **11**, 1421 (1981)].
3. Anan'ev Yu.A. *Laser Resonators and the Beam Divergence Problem* (Bristol: Adam Hilger, 1992; Moscow: Nauka, 1990).
4. Azarova V.V., Golyaev Yu.D., Dmitriev V.G. *Kvantovaya Elektron.*, **30**, 96 (2000) [*Quantum Electron.*, **30**, 96 (2000)].
5. Dorschner T.A. *Proc. SPIE Int. Soc. Opt. Eng.*, **412**, April (1983).
6. Savel'ev I.I., Khromykh A.M. *Kvantovaya Elektron.*, **3**, 1517 (1976) [*Sov. J. Quantum Electron.*, **6**, 821 (1976)].
7. Kudashev V.N., Plachenov A.B., Radin A.M. *Zh. Tekh. Fiz.*, **73**, 111 (2003).
8. Golovin I.V., Kovrigin A.I., Konovalov A.N., Laptev G.D. *Kvantovaya Elektron.*, **22**, 461 (1995) [*Quantum Electron.*, **25**, 436 (1995)].
9. Boiko D.L., Kravtsov N.V. *Kvantovaya Elektron.*, **25**, 880 (1998) [*Quantum Electron.*, **28**, 856 (1998)].
10. Bykov V.P., Silichev O.O. *Lazernye rezonatory* (Laser Resonators) (Moscow: Fizmatlit, 2003).
11. Radina T.V. *Opt. Spektr.*, **80**, 862 (1996).
12. Rudloff R. *IEEE J. Quantum Electron.*, **23**, 438 (1987).
13. Chernen'kii V.I. *Kvantovaya Elektron.*, (5), 53 (1971) [*Sov. J. Quantum Electron.*, **1** (5), 472 (1971)].
14. Aronovits F., in *Primenenie lazerov* (Application of Lasers) (Moscow: Mir, 1974) p. 182.
15. Silichev O.O. *Osnovy optiki gaussovykh puchkov* (Fundamentals of Optics of Gaussian Beams) (Moscow: Moscow Institute of Physics and Technology, 1971).
16. Goncharenko A.M. *Gaussovy puchki sveta* (Gaussian Light Beams) (Moscow: KomKniga, 2005).
17. Gerrard A., Burch J.M. *Introduction to Matrix Methods in Optics* (New York: Wiley, 1975; Moscow: Mir, 1978).
18. Anderson D.Z., Chow W.W., Scully M.O. *Opt. Lett.*, **5**, 413 (1980).